

# Excited-State Intramolecular Hydrogen Atom Transfer and Solvation Dynamics of the Medicinal Pigment Curcumin

Ramkrishna Adhikary,<sup>†</sup> Prasun Mukherjee,<sup>†</sup> Tak W. Kee,<sup>\*,‡</sup> and Jacob W. Petrich<sup>\*,†</sup>

Department of Chemistry, Iowa State University, Ames, Iowa 50011-3111, and School of Chemistry and Physics, University of Adelaide, Adelaide, South Australia, 5005, Australia

Received: November 21, 2008

The potential use of the naturally occurring yellow-orange pigment curcumin as a photodynamic therapy agent is one of the most exciting applications of this medicinal compound. Although subnanosecond spectroscopy has been used to investigate the photophysical processes of curcumin, the time resolution is insufficient to detect important and faster photoinduced processes, including solvation and excited-state intramolecular hydrogen atom transfer (ESIHT). In this study, the excited-state photophysics of curcumin is studied by means of ultrafast fluorescence upconversion spectroscopy. The results show two decay components in the excited-state kinetics with time scales of 12–20 ps and ~100 ps in methanol and ethylene glycol. The resulting prominent isotope effect in the long component upon deuteration indicates that curcumin undergoes ESIHT in these solvents. The short component (12–20 ps) is insensitive to deuteration, and multiwavelength fluorescence upconversion results show that this decay component is due to solvation of excited-state curcumin.

## Introduction

Curcumin, 1,7-bis(4-hydroxy-3-methoxyphenyl)-1,6-heptadiene-3,5-dione, is a naturally occurring yellow-orange pigment derived from the rhizomes of *Curcuma longa* (turmeric). It has been traditionally used as a spice and food coloring in Indian cooking and medicine.<sup>1</sup> Currently, it is the subject of a large number of investigations in the fields of biology, medicine, and pharmacology owing to its profound effects on human health. Curcumin exhibits a variety of biological and photochemical properties, including antioxidant, anti-inflammatory, and anti-cancer activity.<sup>2–6</sup> Recently, it was also established that curcumin has the ability to prevent protein aggregation in debilitating diseases such as Alzheimer's and Parkinson's.<sup>7,8</sup> Curcumin has two tautomeric forms, namely  $\beta$ -diketone and keto–enol. It has been shown that curcumin exists predominantly as a keto–enol tautomer in a number of solvents with various polarities using results from NMR spectroscopy.<sup>9</sup> It follows that strong intramolecular hydrogen bonding is present in the keto–enol tautomer of curcumin, of which the chemical structure is shown in Figure 1, providing a favorable interaction for stabilization of this tautomeric form.

Recent research shows that curcumin has great potential to be an effective photodynamic agent.<sup>10–17</sup> In particular, studies have demonstrated the use of curcumin to treat melanoma,<sup>18–24</sup> and the photodynamic action is greatly enhanced in the presence of light for destruction of tumor cells.<sup>15–17</sup> It has been shown that stable photoproducts are not responsible for the medicinal effects of curcumin.<sup>10</sup> Photolytically produced active oxygen species such as singlet oxygen, hydroxyl radical, superoxide, or hydrogen peroxide are mainly suggested for its activity.<sup>10,11,25–29</sup> In addition, Jovanovich et al. demonstrated that H-atom transfer is a preferred antioxidant mechanism of curcumin by laser flash photolysis and pulse radiolysis.<sup>30</sup> Currently, there are significant

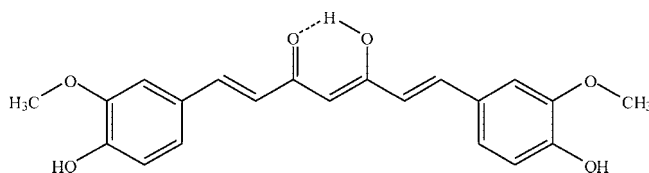


Figure 1. Structure of the keto–enol form of curcumin.

interests in developing a detailed level of understanding in the photophysics and photochemistry of curcumin in order to further exploit its medicinal effects.

Several studies have focused on using time-resolved fluorescence spectroscopy to investigate the excited-state photophysics of curcumin in organic solvents on the subnanosecond time scale, aiming to provide fundamental understanding to elucidate the medicinal properties of curcumin.<sup>12,31–34</sup> In all cases, these studies focused on excited-state intramolecular hydrogen atom transfer (ESIHT) of curcumin because this phenomenon has been associated with the medicinal properties of other pigment molecules, including hypericin and hypocrellin.<sup>35–39</sup> Two of these studies agree that the fluorescence lifetime of curcumin in methanol has a dominant component with a time constant of roughly 130 ps.<sup>31,34</sup> This decay component, however, was assigned to different molecular processes, i.e., solvation<sup>34</sup> and ESIHT,<sup>31</sup> in the two studies. Here, we perform ultrafast fluorescence upconversion studies to address this issue in the literature. Using a time resolution of 300 fs and deuterated curcumin, we show unambiguously that ESIHT occurs with a time scale of approximately 100 ps. Furthermore, the similarity between the time scale of ESIHT and the measured fluorescence lifetime indicates that ESIHT is a major photophysical process in the deactivation of the excited state.

Owing to femtosecond time resolution of ultrafast fluorescence upconversion, a short-lived fluorescence decay component with a time scale of  $12 \pm 2$  ps was also detected at 520 nm for curcumin in methanol, in addition to the ESIHT component. In ethylene glycol, the short-lived component has a time constant of  $20 \pm 3$  ps. This fast decay component was previously

\* To whom correspondence should be addressed. E-mail: tak.kee@adelaide.edu.au (T.W.K.); jwp@iastate.edu (J.W.P.).

<sup>†</sup> Iowa State University.  
<sup>‡</sup> University of Adelaide.

unobserved because of the insufficient time resolution used. Solvation is expected to be present in the relaxation dynamics due to the substantial change in dipole moment reported for curcumin.<sup>31</sup> In the present work, using results from multiwavelength fluorescence upconversion measurements, we definitively assign this decay component to solvation dynamics. The solvation correlation function  $C(t)$ , which provides a quantitative measure of the time scale of solvation dynamics, has a fast component which is shorter than the instrument response function of 300 fs, and a slow component of  $12 \pm 2$  ps in methanol and  $30 \pm 5$  ps in ethylene glycol. These results strongly support the assignment of the 12–20 ps component observed in the fluorescence upconversion results to solvation.

## Experimental Section

**Materials.** Curcumin (purity  $\sim 70\%$  HPLC) was purchased from Sigma Aldrich and used without further purification. High-purity curcumin ( $\geq 98.5\%$ ) was obtained from Alexis Biochemicals. This highly purified product is virtually free of the other two closely related curcuminoids ( $\sim 30\%$ ) which are also found in turmeric, namely demethoxy- and bisdemethoxycurcumin. While the experiments performed in this work involved using curcumin from the first source, fluorescence upconversion and time-correlated single photon counting measurements were repeated using high-purity curcumin to ensure the roles of demethoxy- and bisdemethoxycurcumin are negligible. Methanol, ethylene glycol, and chloroform were obtained from Fisher Scientific and used without further purification. In addition, chloroform was also dried over type 4A molecular sieves prior to use. Methanol- $d_4$  (purity 99.8%) and ethylene glycol- $O,O\text{-}d_2$  (purity 98%) were purchased from Cambridge Isotope Laboratories, Inc. and used without further purification. For the experiments on curcumin in deuterated solvents, curcumin was allowed to equilibrate in these solvents for 48 h to ensure complete exchange of the enolic hydrogen with deuterium.

**Steady-State Measurements.** Steady-state absorption spectra were obtained on Hewlett-Packard 8453 UV–visible spectrophotometer with 1 nm resolution. Steady-state fluorescence spectra were obtained on a Spex Fluoromax-4 with a 3 nm bandpass and corrected for lamp spectral intensity and detector response. All the samples were excited at 407 nm for steady-state fluorescence measurement. For both fluorescence and absorption measurements, a 5 mm path length quartz cuvette was used. All experiments were done at room temperature.

**Time-Resolved Measurements.** The apparatus for fluorescence upconversion is described in detail elsewhere.<sup>40</sup> Briefly it is based on a home-built mode-locked Ti:sapphire oscillator producing femtosecond pulses at a fundamental wavelength of 814 nm with a repetition rate of 82 MHz. Frequency-doubled pulses (407 nm) were used to excite the sample, and the residual of the fundamental was used as the gate pulse to upconvert the fluorescence signal. First, the fluorescence signal was collected using a  $10\times$  objective lens. Then, the gate pulse and fluorescence signal were focused onto a 0.4 mm type-I BBO crystal to generate the sum frequency light, which was detected by a photomultiplier tube mounted on a monochromator. The full width at half-maximum (fwhm) of the instrument response function is 300 fs, obtained by the cross-correlation function of the frequency doubled and the fundamental light. A rotating sample cell was used and all experiments were performed at room temperature.

Solvation dynamics are analyzed and quantified by means of the solvation correlation function,  $C(t)$

$$C(t) = \frac{\nu(t) - \nu(\infty)}{\nu(0) - \nu(\infty)} \quad (1)$$

where  $\nu(0)$ ,  $\nu(t)$ , and  $\nu(\infty)$  denote the peak frequency of the emission spectra at time zero,  $t$ , and infinity. The “zero time” emission spectrum has been approximated using the emission spectrum of curcumin in hexanes, according to the method of Fee and Maroncelli.<sup>41</sup> The  $\nu(\infty)$  is taken as the peak frequency of the steady-state fluorescence spectrum.  $\nu(t)$  is determined by taking the maxima from the log-normal fits as the time-resolved emission maximum which is constructed according to the procedure described by Maroncelli and Fleming<sup>42</sup> using steady-state emission spectrum and fitting parameters from wavelength-resolved decay traces. In most cases, however, the broad spectra result in uncertainty in the exact position of the emission maxima. Thus, using the signal-to-noise ratio and width of the spectrum (including “zero-time”, steady-state, or time-resolved emission spectrum) as guides, we have determined the typical uncertainties as follows: time-resolved emission ( $\sim \pm 200 \text{ cm}^{-1}$ ), “zero-time”  $\sim$  steady state ( $\sim \pm 100 \text{ cm}^{-1}$ ). These uncertainties are used to compute error bars for the  $C(t)$ . The fractional solvation at 300 fs was calculated using  $f_{300\text{fs}} = 1 - C(t=300 \text{ fs})$ .

Time-resolved fluorescence lifetime anisotropy data were collected using the time-correlated single photon counting (TCSPC) technique. Our apparatus has been described elsewhere.<sup>40</sup> Recent modifications in the experimental setup include the replacement of NIM-style electronics by the Becker and Hickl photon counting module Model SPC-630. With this modified system, the full width at half-maximum of the instrument-response function is  $\sim 40\text{--}45$  ps. The acquisition time window had a width of 3.33 ns with 1024 channels, corresponding to 3.25 ps per channel. All experiments were performed using 407 nm excitation obtained by frequency doubling of 814 nm fundamental light. For anisotropy measurements, 65 530 counts were collected at the peak channel for parallel polarization. A normalization factor was then applied to the TCSPC trace such that the maximum count was 10 000 due to requirement of the analysis software. A cuvette of 1 cm path length was used for the time-resolved anisotropy measurement. The anisotropy measurement involved collecting two fluorescence signals with polarizations parallel ( $I_{\parallel}$ ) and perpendicular ( $I_{\perp}$ ) to the excitation polarization in order to determine the anisotropy decay  $r(t)$ , as follows:

$$r(t) = \frac{I_{\parallel}(t) - I_{\perp}(t)}{I_{\parallel}(t) + 2I_{\perp}(t)} \quad (2)$$

The anisotropy data were obtained from simultaneous fitting of parallel and perpendicular decays.<sup>43</sup> The decay of the anisotropy reflects the time scale of orientational relaxation.

## Results and Discussion

**UV–Vis Absorption and Fluorescence Spectra of Curcumin.** Figure 2 illustrates the absorption and fluorescence spectra of curcumin in methanol, ethylene glycol, the corresponding deuterated solvents, and chloroform. The spectra obtained in methanol and chloroform were found to be in agreement with the previous results with respect to the spectral shape and peak position.<sup>33</sup> While the UV–vis absorption spectra are relatively insensitive to the solvent used, the fluorescence spectra exhibit a strong solvent effect. The strong dependence of the Stokes shift on solvent polarity indicates that the excited-

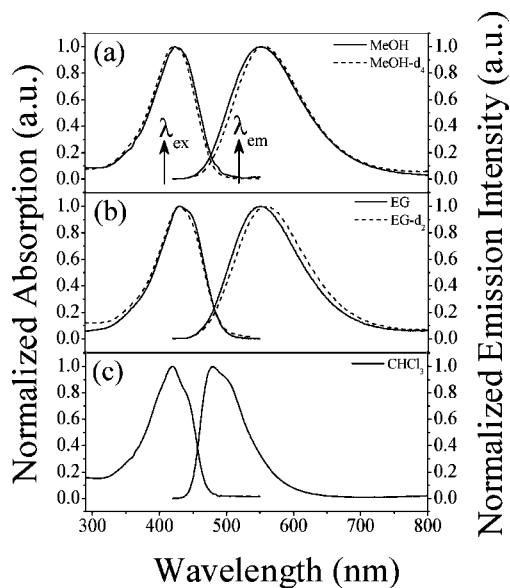


**Figure 2.** Normalized absorption and fluorescence spectra of curcumin in (a) methanol (MeOH), deuterated methanol (MeOH- $d_4$ ), (b) ethylene glycol (EG), deuterated ethylene glycol (EG- $d_2$ ), and (c) chloroform ( $\text{CHCl}_3$ ).

state dipole moment of curcumin is considerably larger than that of its ground state. This property also implies that solvation dynamics play an important role in the excited-state relaxation of curcumin, as will be discussed further.

**Fluorescence Upconversion and Excited-State Intramolecular Hydrogen Atom Transfer of Curcumin.** The excitation and probe wavelengths in the fluorescence upconversion experiments are 407 and 520 nm, respectively, as shown in Figure 2. While having the excitation wavelength at 407 nm efficiently promotes curcumin from the ground state to the excited state, monitoring the time-resolved fluorescence at 520 nm, which is on the blue side of the fluorescence spectrum, provides the good signal-to-noise ratio and sensitivity to record early time events in the excited-state relaxation process.

Figure 3a shows the fluorescence upconversion signals of curcumin in methanol and deuterated methanol as a function of time. The time-resolved fluorescence signal of curcumin in methanol (red) was fitted with a biexponential function with time constants of  $12 \pm 2$  and  $70 \pm 10$  ps with nearly equal amplitudes; see Table 1. In order to demonstrate the effect of deuteration, fluorescence upconversion of curcumin in deuterated methanol was investigated. In deuterated methanol (blue), while the first decay component remains identical within experimental error, a prominent isotope effect is observed in the second component. The decay time constant of this component is increased to  $120 \pm 20$  ps upon deuteration. Fluorescence upconversion experiments were also performed with pure ( $\geq 98.5\%$ ) curcumin in methanol and the same fast and slow components were obtained as mentioned above.

The appearance of this prominent isotope effect of 1.7 requires equilibration of curcumin in deuterated methanol for a period of approximately 48 h. Exchange of the enolic hydrogen of curcumin with the deuterium of methanol- $d_4$  is expected to occur on this time scale, which is consistent with deuteration of a similar system.<sup>44</sup> In contrast, the inset of Figure 3a shows the fluorescence upconversion results of curcumin in methanol and deuterated methanol with an equilibration time of only 15 min. The two traces are identical within experimental error, clearly showing the absence of an isotope effect at early

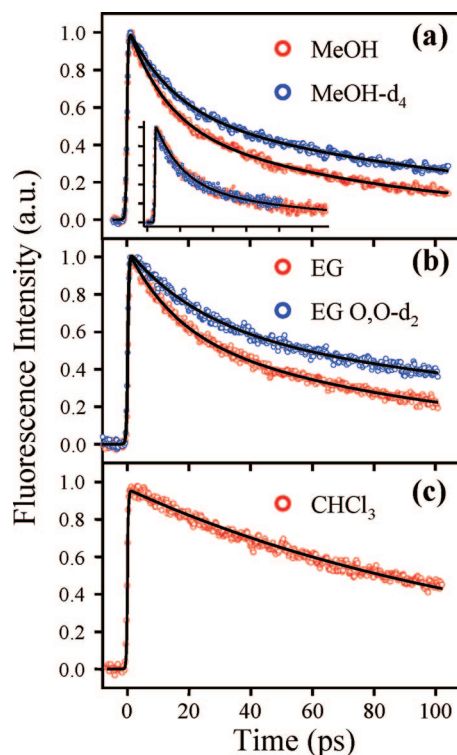


**Figure 3.** Fluorescence upconversion decays of curcumin in (a) methanol (MeOH), (b) ethylene glycol (EG), and (c) chloroform ( $\text{CHCl}_3$ ); corresponding decays in the deuterated analogues in (a) and (b) show a prominent isotope effect. The inset in (a) shows the virtually identical traces prior to the H/D exchange (equilibration time of  $\sim 15$  min), which indicates that the isotope effect observed after equilibration (48 h) is independent of solvent effects. While the decays in (a) and (b) exhibit biexponential nature, the trace in (c) is single exponential. All samples were excited at 407 nm and fluorescence was collected at 520 nm.

**TABLE 1: Fluorescence Upconversion Decay Parameters for Curcumin in Different Solvent Systems<sup>a</sup>**

solvent	$a_1^b$	$\tau_1$ (ps)	$\tau_2$ (ps)
methanol	0.45	12	70
methanol- $d_4$	0.45	12	120
ethylene glycol	0.45	20	105
ethylene glycol- $O,O$ - $d_2$	0.45	20	220
chloroform <sup>c</sup>	1.0	130	—

<sup>a</sup> The fluorescence upconversion traces,  $f(t)$ , were fitted with the multiexponential function  $f(t) = a_1 \exp(-t/\tau_1) + a_2 \exp(-t/\tau_2)$ . The  $a_1$ ,  $a_2$ , and  $\tau_1$  were kept constant during the fitting process. All parameters have a relative error of  $\pm 15\%$ . <sup>b</sup>  $a_1 + a_2 = 1$ . <sup>c</sup> Chloroform was dried over molecular sieves prior to use. Water content was assessed with a coulometric Karl Fischer titration (Mettler Toledo DL 39). % wt  $\text{H}_2\text{O} = 0.002$ .

equilibration time. The results shown in Figure 3a and the inset yield the following important insights. First, the observed isotope effect correlates with the enolic H/D exchange of curcumin, supporting the excited-state hydrogen atom transfer character of the kinetics. Second, the lack of isotope effect at early equilibration time indicates that the hydrogen atom transfer process is intramolecular in nature, as opposed to a consequence of intermolecular hydrogen bonding with the surrounding solvent molecules. Additionally, this result also indicates that the observed isotope effect is unrelated to the suppression of radiationless deactivation of excited-state curcumin in deuterated methanol. Therefore, these results clearly indicate that ESIHT, which occurs with a time constant of 70 ps in methanol, is a major pathway of nonradiative decay in curcumin.



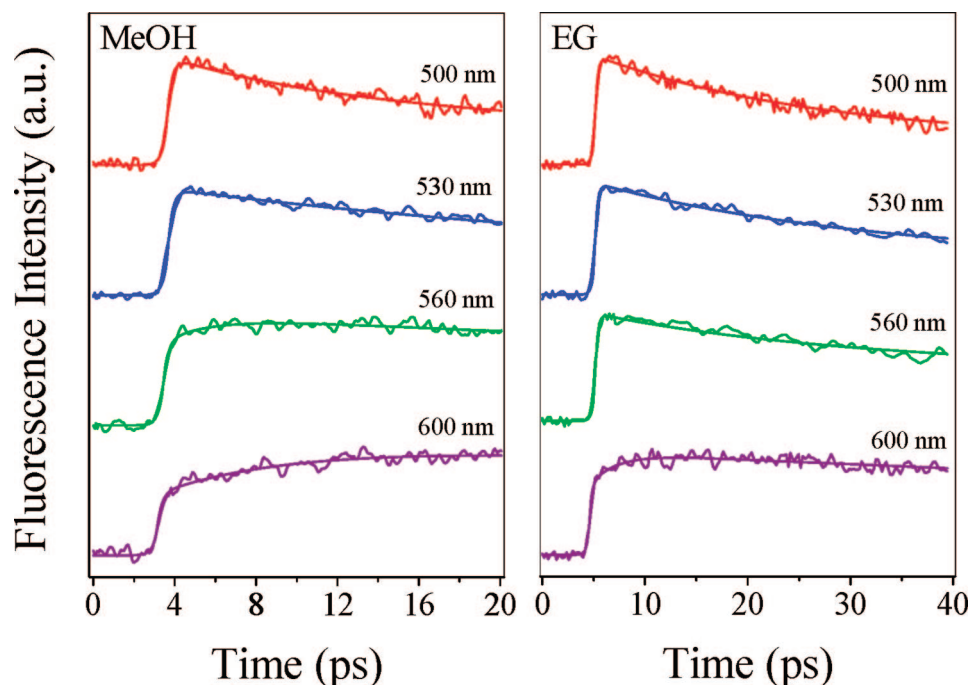


**Figure 4.** Representative normalized wavelength resolved fluorescence upconversion traces of curcumin in methanol (MeOH) and ethylene glycol (EG). Time-resolved emission spectra were constructed by collecting upconversion traces over a range from 500 to 600 nm at intervals of 10 nm. The time-resolved traces at the red end (600 nm) show a growing component, which is the signature of solvation dynamics.

The effect of solvent on the fluorescence upconversion signal is shown in Figure 3b. In ethylene glycol (red), the time-resolved fluorescence signal also exhibits a biexponential decay, similar to methanol. However, the time scales of the decays are longer; the time constants of the decays are  $20 \pm 3$  and  $105 \pm 15$  ps, with nearly equal amplitudes. Deuteration of ethylene glycol produces a similar isotope effect, i.e., the time constant of the short-lived decay component remains unchanged but that of the long-lived component is increased by a factor of 2.1; see Table 1. The presence of this notable effect further supports our assignment of the long-lived decay component to ESIHT. The ESIHT time constants of curcumin reported in this study are comparable to those of 7-azaindole in methanol.<sup>45</sup>

The ESIHT for curcumin in methanol and ethylene glycol occurs, within experimental error, on the same time scale ( $70 \pm 10$  and  $105 \pm 15$  ps, respectively; see Table 1). While the solvent viscosity differs by a factor of  $\sim 30$  between methanol and ethylene glycol (0.59 and 16.1 cP, respectively, at 20 °C), the lack of dependence of the ESIHT time scale on viscosity indicates that ESIHT occurs through small amplitude molecular motions, which do not heavily involve the surrounding solvent molecules. In this regard, ESIHT in curcumin is similar to that in hypericin, for which the rate of ESIHT is uncorrelated to solvent viscosity.<sup>38,39</sup> In another related species, 2-hydroxyacetophenone, it was determined that small-amplitude molecular vibrations are responsible for the initial events in ESIHT and the O–H vibration is unaffected in this process.<sup>46</sup> Therefore, our results indicate that ESIHT in curcumin is similar to that of the systems in which ESIHT has a weak dependence on solvent viscosity.

Chloroform is a polar aprotic solvent with which curcumin is not involved in intermolecular H-bonding. Care was taken to exclude water in chloroform because it has been reported that water quenches the fluorescence by forming a nonfluorescent stable complex with excited-state curcumin.<sup>47</sup> In addition, the presence of a hydrogen-bonding impurity might complicate the excited-state dynamics.<sup>48</sup> The fluorescence upconversion

decay trace of curcumin in chloroform is shown in Figure 3c. The decay trace is best fitted with a single-exponential decay function with a time constant of  $130 \pm 20$  ps. This decay component is assigned to ESIHT for the following reasons. First, the decay trace is unrelated to solvation dynamics of curcumin in chloroform since solvation in chloroform occurs with time constants of 0.285 and 4.15 ps, as determined by Hornig et al.<sup>49</sup> Consequently, because intermolecular hydrogen bonding with the solvent is impossible between curcumin and chloroform, the observed kinetics are attributed to an intramolecular interaction, which we assign to an intramolecular process, namely ESIHT. While the ESIHT time of a related molecule, 3-hydroxyflavone, is 240 fs in methylcyclohexane,<sup>48</sup> the absence of such a short component in Figure 3c indicates that ESIHT in curcumin does not occur as rapidly as in 3-hydroxyflavone. In fact, the 130 ps ESIHT time constant of curcumin in chloroform shows good agreement with those of curcumin in methanol and ethylene glycol.

**Early Time Solvation Dynamics.** In addition to ESIHT, the fluorescence upconversion results also reveal that there is a short-lived component with a time scale of 12 ps in methanol, which is likely to be undetectable in TCSPC because of insufficient time resolution. Solvation, in addition to ESIHT, is expected to play a role in the excited-state relaxation dynamics due to the significant dipole moment change reported for curcumin:  $\Delta\mu = 6.1$  D.<sup>31</sup> Such a  $\Delta\mu$  is comparable to that of Coumarin 153 ( $\Delta\mu \approx 8$  D),<sup>42,49</sup> which is a standard probe molecule for solvation dynamics. Additionally the fluorescence spectra exhibit a Stokes shift that is largely dependent on solvent polarity, implying that solvation may play a major role in the relaxation of the excited state in addition to ESIHT.

To demonstrate the presence of solvation, we performed fluorescence upconversion experiments on curcumin at up to 11 wavelengths spanning the range of 500–600 nm in methanol and ethylene glycol. Representative decay traces are shown in Figure 4. For curcumin in methanol, all the transients are well fitted to a biexponential function with a fixed long decay

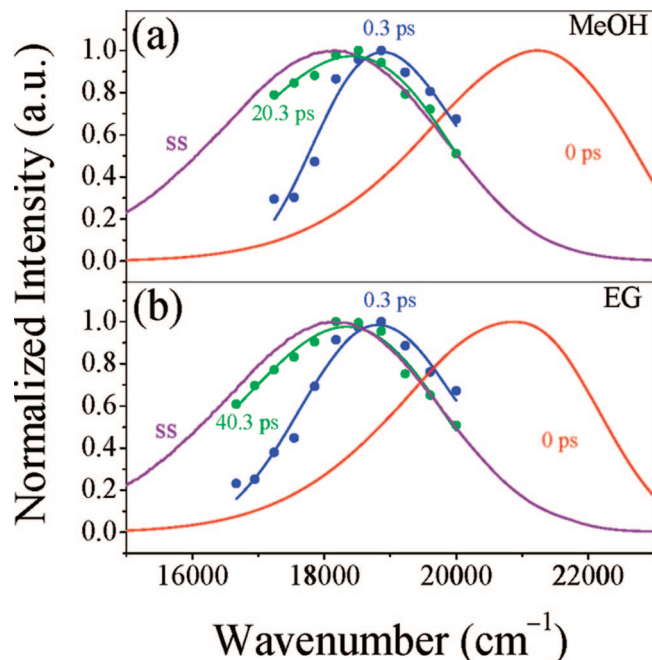


**Figure 5.** Normalized time-resolved emission spectra of curcumin in methanol (MeOH) and ethylene glycol (EG). Steady-state (ss) and “zero-time” ( $t = 0$  ps) spectra are included. Almost 70% of the solvation is complete in both systems within the time resolution of our instrument (300 fs).

component of 140 ps (fluorescence lifetime). In methanol, at the blue end of the emission spectrum (500 nm), the result shows a fast decay component of 10 ps (56%). At 530 nm, the time constant of the fast portion becomes 17 ps (41%). At 560 nm, a rising component is observed with a rise time of 1.6 ps. The time constant of this rising component becomes 6.9 ps at 600 nm. The wavelength-dependent behavior of the fast component is the signature of solvation dynamics. As shown in Figure 4, a similar behavior is also observed for curcumin in ethylene glycol, where the long decay component was also fixed at its lifetime of 210 ps. These results clearly indicate the major role of solvation in the relaxation of the excited state.

In Figure 5a, the emission spectra of curcumin in methanol at 0, 0.3, 20.3 ps and steady state ( $t \rightarrow \infty$ ) are shown. For curcumin in ethylene glycol, the trend of emission spectral shift is similar to methanol but it occurs at a slower rate. For instance, it takes the emission spectrum approximately 40 ps to almost fully recover to the steady-state spectrum, as shown in Figure 5b.

The solvation correlation function,  $C(t)$ , of methanol and ethylene glycol are presented in Figure 6, and the solvation parameters are shown in Table 2. In particular, the  $f_{300\text{fs}}$  values show that more than 70% of solvation is completed in both the solvents within the time resolution (300 fs) of the instrument. The  $C(t)$  shows an initial fast response (50 fs, fixed) followed by a slow response. As shown by previous studies on similar systems, this fast response is attributed to ultrafast librational motion of the solvents.<sup>49–51</sup> The time constants of the other component are  $12 \pm 2$  and  $30 \pm 5$  ps in methanol and ethylene glycol, respectively. These time scales are highly consistent to the fast component in the fluorescence upconversion results at 520 nm of curcumin in these solvents; see Figure 3 and Table 1. Based on the results from the studies on solvation dynamics, the short-lived component in the fluorescence upconversion results for curcumin in methanol and ethylene glycol at 520 nm has been assigned to solvation. In addition, the average

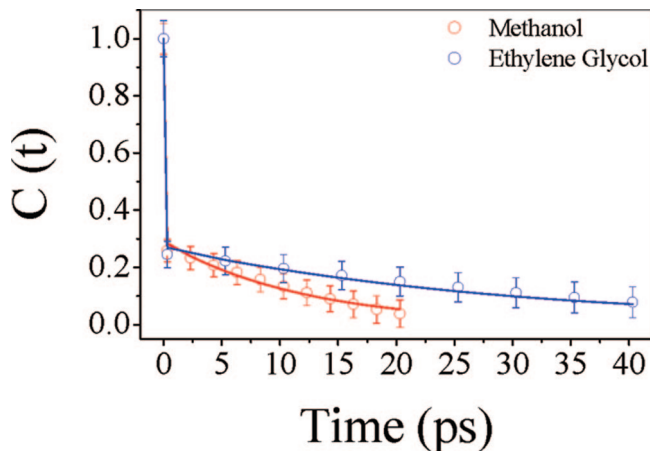


**Figure 6.** Solvation correlation function,  $C(t)$ , of curcumin in methanol and ethylene glycol obtained from fluorescence upconversion experiments. Solvation correlation function is fitted with biexponential decay function. Both the solvents showed the same initial fast component of 50 fs but a different slow component of 12 ps (methanol) and 30 ps (ethylene glycol).

**TABLE 2: Solvation Correlation Function Decay Parameters for Curcumin in Different Solvent Systems**

solvent	$f_{300\text{fs}}^a$	$a_1$	$\tau_1$ (ps) <sup>b</sup>	$\tau_2$ (ps)	$\langle \tau \rangle$ (ps)
methanol	$0.75 \pm 0.04$	$0.71 \pm 0.02$	0.05	$12 \pm 2$	3.5
ethylene glycol	$0.75 \pm 0.05$	$0.73 \pm 0.02$	0.05	$30 \pm 5$	8.2

<sup>a</sup>  $f_{300\text{fs}}$ : fractional solvation at 300 fs. <sup>b</sup> The faster component was fixed at 0.05 ps during fitting.

**TABLE 3: Time-Resolved Fluorescence Anisotropy Data of Curcumin in Different Systems**

system	$r_0$	$\tau^{(r)}$ (ps)	$\tau_{\text{calc}}^{(r)}$ (ps)
curcumin/MeOH <sup>a</sup>	$0.37 \pm 0.01$	$200 \pm 20$	375
curcumin/EG <sup>a</sup>	$0.36 \pm 0.02$	$5080 \pm 1100$	10200

<sup>a</sup> The errors are based on the average of three measurements. Fluorescence anisotropy decays are fitted to the form:  $r(t) = r_0 \exp[-t/\tau^{(r)}]$ . In all cases  $\chi^2 \leq 1.3$ .

solvation times in methanol and ethylene glycol are 3.5 and 8.2 ps, respectively, which are in excellent agreement with previous studies using Coumarin 153 as the probe molecule.<sup>49</sup>

**Fluorescence Anisotropy of Curcumin.** The effects of solvation and ESIHT on the rotational motion of curcumin are examined with fluorescence anisotropy studies. To gain insight into the sensitivity of orientation of curcumin to the environment, anisotropy experiments were carried out in methanol and ethylene glycol, and the results are shown in Figure 7. The anisotropy parameters are shown in Table 3; the anisotropy decays are single exponential, which are well described with the equation  $r(t) = r_0 \exp[-t/\tau^{(r)}]$ , where  $r_0$  and  $\tau^{(r)}$  are the initial anisotropy value and molecular rotational time, respectively. The anisotropy results reveal that  $r_0$  has values of 0.37 and 0.36 in methanol and ethylene glycol, respectively, very close to the theoretical limit of 0.4.

The anisotropy results also reveal that  $\tau^{(r)}$  of curcumin is 200 ps in methanol and 5080 ps in ethylene glycol. The difference between the  $\tau^{(r)}$  of methanol and ethylene glycol can be understood by taking into account the Debye–Stokes–Einstein relation, which states that  $\tau_{\text{DSE}}^{(r)} = V\eta/k_B T$ . Using  $\eta_{\text{methanol}} = 0.59$  cP,  $\eta_{\text{ethylene glycol}} = 16.1$  cP (with  $T = 20$  °C), and the estimated hydrodynamic radius of curcumin of 8.5 Å,<sup>52</sup>  $\tau_{\text{DSE}}^{(r)}$  of methanol and ethylene glycol are estimated to be 375 and 10 200 ps, respectively. Although the Debye–Stokes–Einstein relation

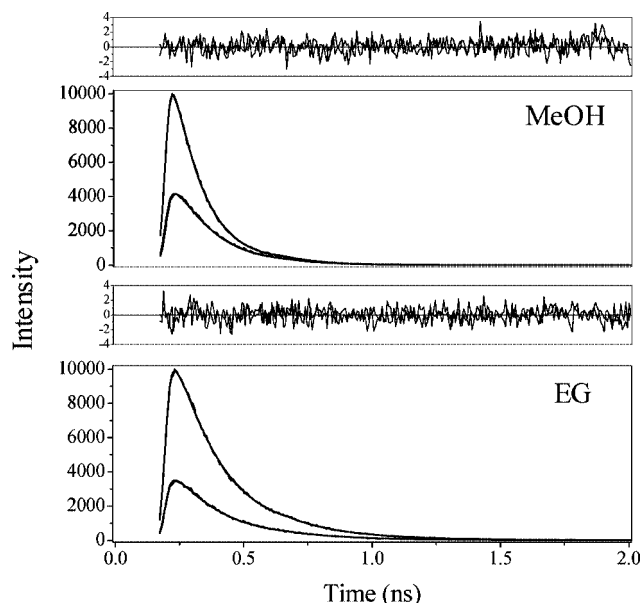


**Figure 7.** Polarized fluorescence traces and residuals of fits for curcumin in methanol (MeOH) and ethylene glycol (EG). Fitting parameters are given in Table 3. The upper trace represents that emission is collected parallel ( $I_{\parallel}$ ) and the lower trace is collected perpendicular ( $I_{\perp}$ ) to the excitation polarization.  $\lambda_{\text{ex}} = 407$  nm,  $\lambda_{\text{em}} \geq 500$  nm.

overestimates  $\tau^{(r)}$  of curcumin for both methanol and ethylene glycol, the ratio between the predicted  $\tau^{(r)}$  agrees very well with the experimental results, indicating, as expected, that viscosity is the determining factor for the molecular rotational time of curcumin.

The comparison between the time scales of molecular rotation and other processes including solvation and ESIHT can provide important insight into the coupling between molecular processes. In the case of curcumin in methanol, we have established that solvation and ESIHT occur on the time scales of 12 and 70 ps, respectively. Relative to the time scale of molecular rotation of 200 ps, the results indicate that the coupling between rotation and either of solvation and ESIHT is weak. Furthermore, the coupling is negligible for curcumin in ethylene glycol. This phenomenon is clearly demonstrated by comparing the molecular rotation time of 5080 ps to the time scales of solvation of 30 ps and ESIHT of 105 ps.

## Conclusion

In summary, we have demonstrated with fluorescence up-conversion that curcumin undergoes excited-state intramolecular hydrogen atom transfer (ESIHT) and it plays a major role in the photophysics of curcumin. Photoexcitation of curcumin produces a fluorescence signal which decays with a biexponential fashion on the order of 12–20 and 70–105 ps. The long-lived signal, which exhibits a prominent isotope effect in deuterated solvents, is attributed to ESIHT. Additionally, the results show that ESIHT is insensitive to solvent viscosity, implying that only small-amplitude motions are coupled to ESIHT of curcumin. We have also presented results from the studies on multiwavelength fluorescence upconversion of curcumin. The results show that only decay components are present in the fluorescence upconversion signals on the blue side of the emission spectrum. A rising component, however, appears on the red side of the emission spectrum, clearly indicating the presence of solvation in the relaxation dynamics. We have shown that curcumin exhibits a long solvation component of

$\sim 12$  ps in methanol and  $\sim 30$  ps in ethylene glycol. Results from fluorescence anisotropy studies show that curcumin in methanol and ethylene glycol have  $\tau^{(r)}$  of 200 and 5080 ps, respectively. By comparing the time scales of solvation and ESIHT with  $\tau^{(r)}$ , we conclude that the coupling between molecular rotation to other molecular processes is weak for curcumin in methanol. Additionally, in the case of curcumin in ethylene glycol, the coupling is essentially negligible.

**Acknowledgment.** T.W.K. acknowledges a research grant from the Australian Research Council and National Health and Medical Research Council Network “Fluorescence Applications in Biotechnology and Life Sciences.”

**Supporting Information Available:** Supplementary UV–vis and TCSPC results. This material is available free of charge via the Internet at <http://pubs.acs.org>.

## References and Notes

- Goel, A.; Kunnumakkara, A. B.; Aggarwal, B. B. *Biochem. Pharmacol.* **2008**, *75*, 787.
- Ruby, A. J.; Kuttan, G.; Babu, K. D.; Rajasekharan, K. N.; Kuttan, R. *Cancer Lett.* **1995**, *94*, 79.
- Lantz, R. C.; Chen, G. J.; Solyom, A. M.; Jolad, S. D.; Timmermann, B. N. *Phytomedicine* **2005**, *12*, 445.
- Aggarwal, B. B.; Kumar, A.; Bharti, A. C. *Anticancer Res.* **2003**, *23*, 363.
- Shi, M.; Cai, Q.; Yao, L.; Mao, Y.; Ming, Y.; Ouyang, G. *Cell Biol. Int.* **2006**, *30*, 221.
- Surh, Y.-J. *Food Chem. Toxicol.* **2002**, *40*, 1091.
- Yang, F.; Lim, G. P.; Begum, A. N.; Ubeda, O. J.; Simmons, M. R.; Ambegaokar, S. S.; Chen, P. P.; Kayed, R.; Glabe, C. G.; Frautschy, S. A.; Cole, G. M. *J. Biol. Chem.* **2005**, *280*, 5892.
- Masuda, M.; Suzuki, N.; Taniguchi, S.; Oikawa, T.; Nonaka, T.; Iwatsubo, T.; Hisanaga, S.-i.; Goedert, M.; Hasegawa, M. *Biochemistry* **2006**, *45*, 6085.
- Payton, F.; Sandusky, P.; Alworth, W. L. *J. Nat. Prod.* **2007**, *70*, 143.
- Tonnesen, H. H.; De Vries, H.; Karlsen, J.; Beijersbergen van Henegouwen, G. *J. Pharm. Sci.* **1987**, *76*, 371.
- Dahl, T. A.; McGowan, W. M.; Shand, M. A.; Srinivasan, V. S. *Arch. Microbiol.* **1989**, *151*, 183.
- Gorman, A. A.; Hamblett, I.; Srinivasan, V. S.; Wood, P. D. *Photochem. Photobiol.* **1994**, *59*, 389.
- Chignell, C. F.; Bilski, P.; Reszka, K. J.; Motten, A. G.; Sik, R. H.; Dahl, T. A. *Photochem. Photobiol.* **1994**, *59*, 295.
- Dahl, T. A.; Bilski, P.; Reszka, K. J.; Chignell, C. F. *Photochem. Photobiol.* **1994**, *59*, 290.
- Chan, W.-H.; Wu, H.-J. *J. Cell. Biochem.* **2004**, *92*, 200.
- Koon, H.; Leung, A. W. N.; Yue, K. K. M.; Mak, N. K. *J. Environ. Pathol. Toxicol. Oncol.* **2006**, *25*, 205.
- Park, K.; Lee, J.-H. *Oncol. Rep.* **2007**, *17*, 537.
- Menon, L. G.; Kuttan, R.; Kuttan, G. *Cancer Lett.* **1995**, *95*, 221.
- Iersel, M. L.; Ploemen, J.-P.; Struik, I.; Amersfoort, C. v.; Keyzer, A. E.; Schefferlie, J. G.; Bladeren, P. J. v. *Chem. Biol. Interact.* **1996**, *102*, 117.
- Odot, J.; Albert, P.; Carlier, A.; Tarpin, M.; Devy, J.; Madoulet, C. *Int. J. Cancer* **2004**, *111*, 381.
- Zheng, M.; Ekmekcioglu, S.; Walch, E. T.; Tang, C.-H.; Grimm, E. A. *Melanoma Res.* **2004**, *14*, 165.
- Siwak, D. R.; Shishodia, S.; Aggarwal, B. B.; Kurzrock, R. *Cancer* **2005**, *104*, 879.
- Lao, C. D.; Demierre, M.-F.; Sondak, V. K. *Expert Rev. Anticancer Ther.* **2006**, *6*, 1559.
- Marin, Y. E.; Wall, B. A.; Wang, S.; Namkoong, J.; Martino, J. J.; Suh, J.; Lee, H. J.; Rabson, A. B.; Yang, C. S.; Chen, S.; Ryu, J.-H. *Melanoma Res.* **2007**, *17*, 274.
- Sharma, O. P. *Biochem. Pharmacol.* **1976**, *25*, 1811.
- Priyadarsini, K. I. *Free Radical Biol. Med.* **1997**, *23*, 838.
- Khopde, S. M.; Priyadarsini, K. I.; Venkatesan, P.; Rao, M. N. A. *Biophys. Chem.* **1999**, *80*, 85.
- Kunchandy, E.; Rao, M. N. A. *Int. J. Pharm.* **1989**, *57*, 173.
- Kunchandy, E.; Rao, M. N. A. *Int. J. Pharm.* **1990**, *58*, 237.
- Jovanovic, S. V.; Steenken, S.; Boone, C. W.; Simic, M. G. *J. Am. Chem. Soc.* **1999**, *121*, 9677.
- Khopde, S. M.; Priyadarsini, K. I.; Palit, D. K.; Mukherjee, T. *Photochem. Photobiol.* **2000**, *72*, 625.

- (32) Barik, A.; Priyadarsini, K. I.; Mohan, H. *Orient. J. Chem.* **2002**, *18*, 427.
- (33) Barik, A.; Goel, N. K.; Priyadarsini, K. I.; Mohan, H. *J. Photosci.* **2004**, *11*, 95.
- (34) Nardo, L.; Paderno, R.; Andreoni, A.; Masson, M.; Haukvik, T.; Tonnesen, H. H. *Spectroscopy* **2008**, *22*, 187.
- (35) Das, K.; English, D. S.; Petrich, J. W. *J. Phys. Chem. A* **1997**, *101*, 3241.
- (36) English, D. S.; Zhang, W.; Kraus, G. A.; Petrich, J. W. *J. Am. Chem. Soc.* **1997**, *119*, 2980.
- (37) Smirnov, A. V.; Das, K.; English, D. S.; Wan, Z.; Kraus, G. A.; Petrich, J. W. *J. Phys. Chem. A* **1999**, *103*, 7949.
- (38) Das, K.; English, D. S.; Petrich, J. W. *J. Am. Chem. Soc.* **1997**, *119*, 2763.
- (39) Petrich, J. W. *Int. Rev. Phys. Chem.* **2000**, *19*, 479.
- (40) Chowdhury, P. K.; Halder, M.; Sanders, L.; Calhoun, T.; Anderson, J. L.; Armstrong, D. W.; Song, X.; Petrich, J. W. *J. Phys. Chem. B* **2004**, *108*, 10245.
- (41) Fee, R. S.; Maroncelli, M. *Chem. Phys.* **1994**, *183*, 235.
- (42) Maroncelli, M.; Fleming, G. R. *J. Chem. Phys.* **1987**, *86*, 6221.
- (43) Cross, A. J.; Fleming, G. R. *Biophys. J.* **1984**, *46*, 45.
- (44) Fita, P.; Urbanska, N.; Radzewicz, C.; Waluk, J. Z. *Phys. Chem.* **2008**, *222*, 1165.
- (45) Moog, R. S.; Maroncelli, M. *J. Phys. Chem.* **1991**, *95*, 10359.
- (46) Peteanu, L. A.; Mathies, R. A. *J. Phys. Chem.* **1992**, *96*, 6910.
- (47) Bong, P.-H. *Bull. Korean Chem. Soc.* **2000**, *21*, 81.
- (48) Schwartz, B. J.; Peteanu, L. A.; Harris, C. B. *J. Phys. Chem.* **1992**, *96*, 3591.
- (49) Horng, M. L.; Gardecki, J. A.; Papazyan, A.; Maroncelli, M. *J. Phys. Chem.* **1995**, *99*, 17311.
- (50) Jimenez, R.; Fleming, G. R.; Kumar, V. P.; Maroncelli, M. *Nature* **1994**, *369*, 471.
- (51) Fleming, G. R.; Cho, M. *Annu. Rev. Phys. Chem.* **1996**, *47*, 109.
- (52) Zsila, F.; Bikadi, Z.; Simonyi, M. *Org. Biomol. Chem.* **2004**, *2*, 2902.

JP901234Z